JOURNAL OF SOLID STATE CHEMISTRY 63, 369–376 (1986)

Phase Relations and Structure of $V_{3-x}Mo_xS_4$ ($0 \leq x \leq 2$)

HIROAKI WADA, MITSUKO ONODA, HIROSHI NOZAKI, AND ISAO KAWADA†

National Institute for Research in Inorganic Materials, 1-1 Namiki, Sakura-Mura, Niihari-Gun, Ibaraki, Japan 305

Received July 1, 1985; in revised form November 22, 1985

Phase relations, composition dependence of lattice constants, structure refinement, and electrical resistivity of the mixed-metal compounds, $(V,Mo)_3S_4$, are presented. Phase relationships in the system V–Mo–S were studied by sealed silica tube experiments at 1373 K and an isothermal section of the phase diagram was constructed. The system V–Mo–S is characterized by the following three solid solution series: cubic metal alloy V_xMo_{1-x} ($0 \leq x \leq 1$), monoclinic $(V_xMo_{1-x})_{2.06}S_3$ ($0 \leq x \leq 0.06$), and monoclinic $V_{3-x}Mo_xS_4$ ($0 \leq x \leq 2$). The $(V,Mo)_3S_4$ phase coexists with MoS_2 at higher S content, while it coexists with Mo at lower S content. The structures of VMo_2S_4 and V_2MoS_4 were determined and refined from X-ray powder data. A monoclinic Cr_3S_4-type cell with space group $I2/m$ was adopted. It was found that the contraction of the lattice constant b on substitution of Mo for V in $(V,Mo)_3S_4$ mixed crystals is due to formation of characteristic zigzag Mo–Mo chains running along the b direction of the lattice. With respect to the metal distribution of Mo and V in the Cr_3S_4-type structure, Mo atoms have a great tendency to occupy metal sites in the metal-filled layers rather than those in the metal-deficient layers.

Introduction

Ternary molybdenum sulfides with the general formula MMo_2S_4 (M = V, Cr, Fe, and Co) crystallize in the monoclinic space groups $C2/m$ or Cc, in which Mo and M atoms occupy octahedral holes in hexagonal close packed sulfur slabs (*1–3*). These structures are characterized by the existence of a M–S–Mo–S–M layer sequence along the a or c direction and can be closely related to the Cr_3S_4-type cell with the space group $I2/m$ (an unreduced presentation of $C2/m$), intermediate between the NiAs and $Cd(OH)_2$ types, or its modifications. X-Ray single-crystal analyses and measurements of the electrical resistivity, the magnetic susceptibility, and the thermoelectric power on these compounds have yielded much information about their lattice and physical properties (*4–6*). However, little is known about their phase relations and the precise shape of their phase regions. It is therefore of special importance to establish the phase diagrams of the M–Mo–S system from the thermodynamical point of view.

We reported the phase relations of Fe-Chevrel compounds and the phase diagrams of the system Fe–Mo–S at 1273 K in the previous paper (*7*). The V–Mo–S system was chosen as a further subject in order to examine the mutual solubility between the V–S and Mo–S systems. In the course of the continuing study of the V–Mo–S sys-

† Deceased.

0022-4596/86 $3.00

tem at 1373 K, we found a $(V,Mo)_3S_4$ solid solution with the Cr_3S_4-type structure in which two kinds of crystallographically different metal sites exist. Recent crystal chemical studies on the metal distribution in the Cr_3S_4 lattice (*8–10*) led us to investigate $(V,Mo)_3S_4$ compounds by X-ray powder analyses.

In this paper we describe the phase relations of the system V–Mo–S at 1373 K, the structure refinement and the electrical resistivity of $(V,Mo)_3S_4$ compounds.

Experimental

For the preparation of ternary sulfides, molybdenum (3N6), vanadium (2N5), and sulfur (6N) powders were used as starting materials. Initially, MoS_2 and V_3S_4 were prepared from these elements at 1373 and 1273 K, respectively, and employed as source materials throughout all of the experiments. The samples were prepared by weighing these source materials individually in the desired proportions to an accuracy of 0.1 mg. The ingredients were mixed in an agate mortar, pressed into pellet, and sealed in evacuated silica tubes at less than 10^{-3} Torr. The heat treatments were carried out at 1373 K for 4 to 7 days and then the tubes were quenched in water. The composition of binary sulfides and metal was determined by weight loss and gain method on oxidation to MoO_3 and V_2O_5. Overall errors in the compositions were determined to be less than 0.2 wt%.

The phase characterization was made by reflected-light microscopy, electron and X-ray powder diffraction methods. X-ray intensity data were measured by θ–2θ scanning on a Rigaku diffractometer (Geigerflex, RAD-2B system) using graphite-monochromated Cu $K\alpha$ radiation. The lattice parameters of the monoclinic phases were calculated using the least-squares method of UNICS, RSLC-3 (*11*). Structural parameters were determined through the refinement treatment by means of a computer program PPRG (*12*).

The electrical resistivity of vanadium molybdenum sulfide was measured on a sintered pellet using a dc four-probe method in a helium atmosphere. The pellet was formed from powders by pressing with a pressure of 2 tons/cm^2 at room temperature, annealing in an evacuated silica tube for 5 hr at 1773 K, and subsequent quenching. The electrical contacts of a pellet (2.8 × 1.85 × 0.75 mm) were made with a silver paint.

Results and Discussion

Phase Relations of the V–Mo–S System at 1373 K

The isothermal section of phase diagrams of the V–Mo–S system at 1373 K was constructed on the basis of our experimental results and from the binary Mo–S (*13*), V–S (*14–16*), and Mo–V phase diagrams (*17*). The phase relationships in the section are shown in Fig. 1 together with our experimental data. The boundary between phase assemblages is determined mainly by X-ray diffraction of quenched samples with different compositions.

In the Mo–V system, only the cubic metallic solid solution phase was confirmed to be stable in the whole compositional range. Slight positive deviation of the lattice constant a from Vegard's rule was observed at compositions near the V metal. The lattice constant of $V_{0.9}Mo_{0.1}$ alloy was found to be $a = 3.051$ Å.

In the Mo–S system, hexagonal MoS_2 and monoclinic Mo_2S_3 exist at 1373 K. The former has the stoichiometric composition, but the latter has a nonstoichiometric one rich in Mo metal. The homogeneity range of Mo_2S_3 extends from $MoS_{1.456}$ to $MoS_{1.475}$, as reported previously (*7*).

In the V–S system, monoclinic V_3S_4, pseudo-hexagonal $V_{1-x}S$, orthorhombic

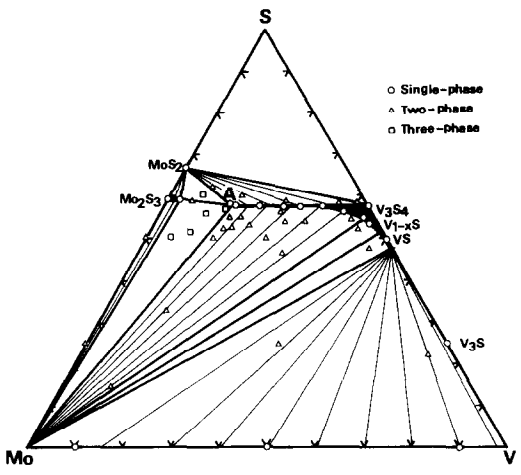

FIG. 1. Isothermal section of the phase diagram of the V–Mo–S system at 1373 K. The positions of most of the tie lines in divariant regions are drawn arbitrarily. Composition A represents VMo_2S_4, one of the end members of the $(V,Mo)_3S_4$ solid solution.

MnP-type VS and tetragonal α-V_3S are found from X-ray diffractograms of quenched samples. These phase relations, however, do not always reflect the products of equilibration at 1373 K because there is a possibility of phase changes occurring during the quenching process due to phase transition and decomposition. So, prior to the construction of the phase diagrams, particular attention should be given to the nonquenchable character of the high temperature phases in the V–S system.

The phase transformation of orthorhombic MnP-type VS to hexagonal NiAs-type VS was first observed by Franzen and Wiegers (*18*) by means of DTA and high-temperature X-ray diffraction. According to De Vries and Jellinek (*16*), this transition occurs at about 873 K for $VS_{1.00}$ and at about 623 K for $VS_{1.05}$. These facts mean clearly that NiAs-type VS is stable at 1373 K. This phase, however, is not quenchable to room temperature, so that only MnP-type VS is observed as a stable phase. Oka *et al.* (*19*) studied the vacancy order–disorder transition of the V–S system by means of high-temperature X-ray diffraction method and found that the phase transition from V_3S_4 to the NiAs type occurs above 1473 K. Based on these findings, the following phase relations at 1373 K are derived: tetragonal α-V_3S, hexagonal VS (range $VS_{0.93}$–$VS_{1.06}$), pseudo-hexagonal $V_{1-x}S$ (range $VS_{1.06}$–$VS_{1.18}$), and monoclinic V_3S_4 (range $VS_{1.20}$–$VS_{1.34}$). Besides the binary phases described above, we confirmed the two solid solution series in the V–Mo–S system: monoclinic $V_{3-x}Mo_xS_4$ ($0 \leq x \leq 2$) and monoclinic $(V_xMo_{1-x})_{2.06}S_3$ ($0 \leq x \leq 0.06$). With respect to the sulfur content, the former has the very narrow compositional range from 57 to 58 at.% of S over a range of the ratio Mo/V between $\frac{1}{2}$ and 2, suggesting that the metal to sulfur ratio is invariantly 3 : 4. As shown in Fig. 1, however, the homogeneity range of the $(V,Mo)_3S_4$ phase broadens rapidly near the binary V–S. The lattice parameters of $(V_{0.06}Mo_{0.94})_{2.06}S_3$ located at the phase limit of the latter at 1373 K were found to be a = 6.091 Å, b = 3.211 Å, c = 8.602 Å, β = 102.71°.

The lattice parameters of the monoclinic $(Mo,V)_3S_4$ phase are shown as a function of the composition in Fig. 2. It should be noted that Vegard's rule is not obeyed in this system. The lattice constants, a, c, and β, and the unit cell volume V increase with increasing Mo content, while b decreases. The volume of the unit cell changes by about 2% within the whole solid solution range. A possible explanation for the increase of the lattice constants, a, c, and V, is the size effect on replacing the smaller V atoms (atomic radius 1.34 Å) by larger Mo atoms (atomic radius 1.39 Å) in V_3S_4 with the Cr_3S_4-type structure. On the other hand, the variation of the lattice constant b can be explained by the Mo–Mo zigzag chain formation and the subsequent contraction of the b axis, in the same way as in $Mo_{2.06}S_3$ (*21*).

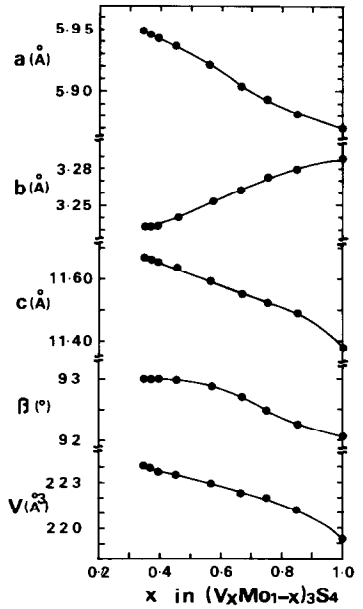

FIG. 2. Variation of the lattice parameters, a, b, c, β, and V with x in $(V_xMo_{1-x})_3S_4$ quenched from 1373 K.

Structure of VMo_2S_4 and V_2MoS_4

All peaks in the diffractograms of VMo_2S_4 could be indexed by means of a monoclinic unit cell with a = 5.949(1) Å, b = 3.236(1) Å, c = 11.670(4) Å, β = 92.91(2)°, V = 224.4(1) Å^3. Since only X-ray reflections with $h + k + l = 2n$ were observed, the structure of Cr_3S_4-type with space group $I2/m - C_{2h}^3$ was adopted for this compound. In this structure, the sulfur atoms are arranged in a hexagonal close packing of the type *ABAB* (Fig. 3). Two metal sites, M_I in metal-vacant layers and M_{II} in metal-filled layers, exist in the octahedral holes of the sulfur packing in an ordered fashion.

The x and z parameters and isotropic temperature factors were refined starting from the parameters of V_3S_4 reported by De Vries and Jellinek (*16*). The values of these parameters were adjusted to minimize the sum of the squares of the differences between observed and calculated intensities of the selected 23 unambiguous and 8 overlapping reflections. The measure of agreement of observed and calculated X-ray diffraction intensities is afforded by the disagreement index R

$$R = \Sigma|I_{obs} - I_{calc}|/\Sigma I_{obs}.$$

Intensities of reflections were calculated on the basis of the following three models of metal distributions: (A) all Mo atoms occupy preferentially M_{II} sites of metal-filled layers, (B) Mo and V atoms are distributed statistically at random on both sites, M_I and M_{II}, and (C) all V and half of Mo atoms occupy M_{II} sites, but are randomly distributed within these layers. After several cycles of refinement for model A, the final R value converged at 0.072 for the observed intensities, while R values for models B and C were 0.55 and 0.65, respectively. This suggests clearly that model A is correct for the structure of VMo_2S_4. Final values of all

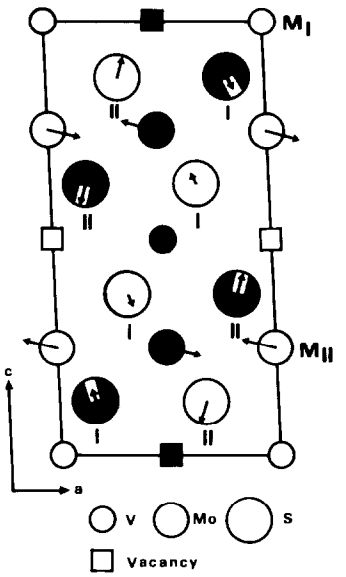

FIG. 3. Structure of monoclinic VMo_2S_4 projected on the (010) plane. Dark circles represent atoms at y = ½. Open circles represent atoms at y = 0. The displacements of the atoms from their ideal positions are indicated by arrows (two times enlarged). I and II distinguish the crystallographically independent sets of sulfur atoms.

TABLE I

ATOMIC COORDINATES AND ISOTROPIC THERMAL PARAMETERS OF VMo_2S_4[a]

Atom	Position	x	y	z	B (Å^2)
V	2(*a*)	0.0	0.0	0.0	0.91(25)
Mo	4(*i*)	0.9465(6)	0.0	0.2561(4)	0.98(11)
S_I	4(*i*)	0.3401(15)	0.0	0.3675(3)	0.76(33)
S_{II}	4(*i*)	0.3431(17)	0.0	0.8938(4)	0.88(30)

[a] Standard deviations in units of the last decimal are given in parentheses.

structural parameters are given in Table I. Table II contains the observed and calculated intensities derived from these parameters. Interatomic distances are listed in Table III. Standard deviations in distances range from 0.011 Å for S–S to 0.006 Å for Mo–Mo. The final structure is shown in Fig. 3. Mo atoms occupying M_{II} sites are displaced from the octahedral centers in such a way that infinite zigzag chains are formed running in the b direction. The characteristic features of the chain formation in M_{II} layers are represented in Fig. 4. The Mo–Mo distances in these chains are 2.841 Å, which is comparable to the distances of 2.86 Å in $Mo_{2.06}S_3$ (*21*) and the average 2.852 Å in $CoMo_2S_4$ (*3*). The shortest distance between the chains is 3.967 Å. The average V–S and Mo–S bond lengths, 2.414 and 2.479 Å, in VMo_2S_4 are close to the corresponding lengths of 2.406 Å in V_3S_4 (*20*) and 2.456 Å in $CoMo_2S_4$. The interlayer V–Mo lengths, 3.022 Å, are slightly longer than the corresponding V–V distances, 2.919 Å, in V_3S_4.

A few remarks should be made here regarding the character of the bond involved in VMo_2S_4. Chevrel *et al.* (*4*) first reported that V atoms exist as V^{2+} from susceptibility measurement. The unit cell volume of VMo_2S_4 is about 1% smaller than that of $CrMo_2S_4$ which has localized 3*d* electrons. If one assumes ionic models, however, VMo_2S_4 should have larger volume than $CrMo_2S_4$ because V^{2+} is larger than Cr^{2+}.

TABLE II

COMPARISON OF THE CALCULATED AND OBSERVED INTENSITIES OF X-RAY DIFFRACTOGRAMS OF VMo_2S_4

h k l	Cu$K\alpha$ 2θ (obs)	I_{calc}	I_{obs}
0 0 2	15.19	100	100
1 0 1	17.09	38	39
−1 0 3	26.79	16	17
0 1 1	28.63	6	7
2 0 0	30.12	23	18
0 0 4	30.71	14	12
1 1 0	31.49	49	43
2 0 2	34.57	37	36
−1 1 2	34.78	80	80
0 1 3	36.14	12	16
−1 0 5	40.91	2	2
−2 1 1	41.74	6	4
2 1 1 −2 0 4 1 0 5	42.37	51	52
−1 1 4	43.98	50	57
2 0 4	44.69	20	24
1 1 4	45.13	63	62
−3 0 1	46.15	4	2
0 0 6 −2 1 3 3 0 1	46.76	41	42
2 1 3	48.54	3	3
−3 0 3	50.73	13	14
3 1 0	54.36	25	31
−2 0 6	55.22	4	4
−2 1 5 −1 0 7 −1 1 6 0 2 0	56.60	27	29
2 0 6 1 1 6 1 0 7	58.03	13	14
2 1 5	58.95	3	2
0 2 2	59.26	5	4
−1 2 1 −3 0 5 1 2 1	59.64	6	4
−4 0 2 0 0 8 −1 2 3	63.94	13	13
4 0 2 2 2 0	65.64	4	5
2 2 2	68.36	8	8
−4 0 4 −2 1 7	69.56	10	10

TABLE III

INTERATOMIC DISTANCES IN ANGSTROMS FOR VMo_2S_4[a]

V–V, Mo–Mo(=*b*): 3.236	S_I–S_{II}: 3.398, 3.402, 3.446, 3.665
Mo–V: 3.022	Around each S_I
Mo–Mo: 2.841, 3.967	2S–V: 2.401
V–S_I: 2.401	2S–Mo: 2.620
V–S_{II}: 2.441	1S–Mo: 2.549
Mo–S_I: 2.549, 2.620	Around each S_{II}
Mo–S_{II}: 2.383, 2.392	2S–Mo: 2.383
S_I–S_I: 3.236, 3.315, 3.548	1S–Mo: 2.392
S_{II}–S_{II}: 3.027, 3.236, 3.838	1S–V: 2.441

[a] V–S average, 2.414 Å; Mo–S average, 2.479 Å.

This discrepancy may be explained partly by the electron delocalization effect owing to the direct overlap of *d* orbitals of adjacent V atoms, as is the case for binary vanadium–sulfide compounds (*22*). It is well known that the metal–sulfur bond length is characteristic of the metal oxidation state (*23, 24*). Comparison of bond length of VMo_2S_4 with the corresponding Fe sulfides provides us some more information about it. The average Fe–S bond length in $FeMo_2S_4$ is 2.41 Å (*3*), which is comparable to that of V–S in VMo_2S_4. According to Fatseas *et al.* (*25*), Fe in $FeMo_2S_4$ exists as Fe^{2+} with high spin, so that the corresponding ionic formula can be written as $Fe^{2+}Mo_2^{3+}S_4^{2-}$. In an ionic model, the V–S bond length should be larger than that of Fe–S. However, this is not the case for VMo_2S_4. The contraction of V–S distances may be due to the covalence effects.

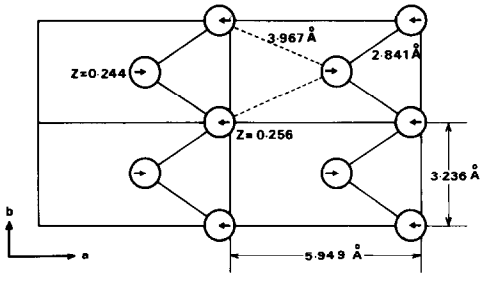

FIG. 4. Molybdenum atoms near the plane $z = \frac{1}{4}$ projected on that plane. Arrows indicate the displacements of the atoms from their ideal positions.

A similar procedure was applied to refine the structure of V_2MoS_4 with the lattice constant: $a = 5.902(1)$ Å, $b = 3.262(1)$ Å, $c = 11.550(2)$ Å, $\beta = 92.65(1)°$; $V = 222.1(1)$ Å^3. The good agreement of calculated and observed intensities of reflection was obtained under the condition that all Mo and half of the V atoms occupy M_{II} sites of metal-filled layers, but are randomly distributed within these layers. The final *R* value converged at 0.078. The positional parameters of V_2MoS_4 are listed in Table IV. In addition, a similar type of metal distribution in the lattice was confirmed for $(V_{0.75}Mo_{0.25})_3S_4$ ($R = 0.09$). To clarify the structural change in the V_3S_4–VMo_2S_4 series, the deviation of the observed positional parameters of atoms from ideal was calculated using the structural data ob-

TABLE IV

ATOMIC COORDINATES AND ISOTROPIC THERMAL PARAMETERS OF V_2MoS_4

Atom	Position	*x*	*y*	*z*	*B* (Å^2)
V_I	2(*a*)	0.0	0.0	0.0	0.99(20)
V_{II} } Mo	4(*i*)	0.9475(6)	0.0	0.2572(5)	1.00(86) / 0.99(42)
S_I	4(*i*)	0.3413(15)	0.0	0.3665(5)	1.04(35)
S_{II}	4(*i*)	0.3418(16)	0.0	0.8930(5)	0.82(31)

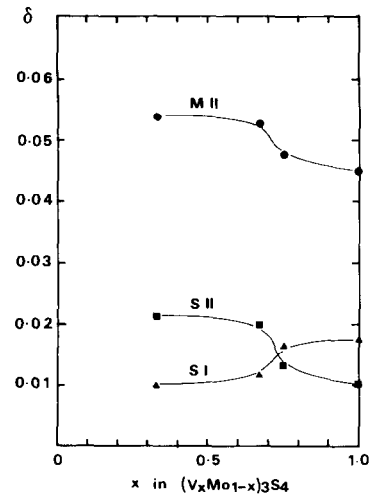

FIG. 5. Relation of composition with the positional deviation, δ.

tained through the refinement. The following equations are used for the explanation of deviation: $\delta^2_{M_{II}} = (1 - x_{M_{II}})^2 + (\frac{1}{4} - z_{M_{II}})^2$; $\delta^2_{S_I} = (\frac{1}{8} - x_{S_I})^2 + (\frac{3}{8} - X_{S_I})^2$; $\delta^2_{S_{II}} = (\frac{1}{3} - x_{S_{II}})^2 + (\frac{7}{8} - z_{S_{II}})^2$. Figure 5 shows the relation of composition with δ. A change in the δ values as a function of composition in V_3S_4–VMo_2S_4 solid solution series seems to occur regularly with changes in lattice constant. The value of $\delta_{M_{II}}$ increases from 0.045 to 0.054 with increasing Mo content. However, it should be noted that δ_{S_I} decreases with increasing Mo content, while $\delta_{S_{II}}$ increases and δ_{S_I} and $\delta_{S_{II}}$ curves intersect at about $x = 0.7$, where the curvature changes.

With respect to site preference of metal atoms in Cr_3S_4-type $(V,Mo)_3S_4$ solid solutions, Mo atoms have the great tendency to occupy the M_{II} site rather than the M_I site. Recently Ueda *et al.* (*8*) have studied the metal distribution of Cr_3S_4-type transition metal chalcogenides and classified $(M',M)_3X_4$ solid solutions into three types in terms of site preference of metal atoms:

(a) $(M'_{3x}M_{1-3x})[M_2]S_4$ $\quad 0 \le x \le \frac{1}{3}$

$(M')[M'_{3x-1}M_{3-3x}]S_4$ $\quad \frac{1}{3} \le x \le 1$

(b) $(M)[M'_{3x}M_{2-3x}]S_4$ $\quad 0 \le x \le \frac{2}{3}$

$(M'_{3x-2}M_{3-3x})[M'_2]S_4$ $\quad \frac{2}{3} \le x \le 1$

(c) $(M'_xM_{1-x})[M'_{2x}M_{2-2x}]S_4$ $\quad 0 \le x \le 1$,

where parentheses and brackets correspond to site I and site II of metal atoms, respectively. In the case of $(V,Mo)_3S_4$ solid solutions the substitution mode of metal atoms belongs to the (b) type, $(V)[Mo_{3x}V_{2-3x}]S_4$ $(0 \le x \le \frac{2}{3})$ in going from V_3S_4 to VMo_2S_4.

Electrical Resistivity of $(V_{0.347}Mo_{0.634})_3S_4$

No indications for a superconductor were found down to liquid helium temperature, 4.2 K. As shown in Fig. 6, a plot of the resistivity ρ vs T for $(V_{0.347}Mo_{0.634})_3S_4$ reflects a semiconducting behavior with an activation energy of 9.4×10^{-5} eV at lower temperatures. The resistivity changes from 5.9×10^{-3} Ω cm at room temperature to 1.7×10^{-2} Ω cm at liquid helium temperature, having a slight broad minimum with 5.7×10^{-3} Ω cm at about 180 K. An appreciable hysteresis between resistivities on heating and on cooling is also observed. It should be noted that the resistivity of our sample is lower by one order of magnitude than that

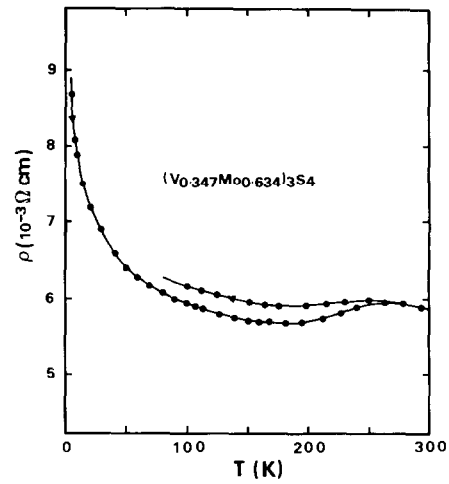

FIG. 6. Electrical resistivity ρ as a function of the temperature.

of VMo_2S_4 reported by Chevrel *et al.* (*4*). The appearance of a minimum on the resistivity curves may be considered to reflect a structural phase transition similar to that for $Mo_{2.06}S_3$ which has been described by De Jonge *et al.* (*21*). Judging from the similarity in the electrical resistivities of both compounds, the phenomenon may be interpreted as being closely related to the inherent feature of chemical bonding of Mo atoms, such as formation of Mo–Mo zigzag chains in the lattice. A large single crystal would be necessary for a better understanding of the phase transition and electrical properties of the $(V,Mo)_3S_4$ phase.

References

1. K. Anzenhofer and J. J. De Boer, *Acta Crystallogr. Sect. B* **25,** 1419 (1969).
2. J. Guillevic, R. Chevrel, M. Sergent, and D. Grandjean, *Bull. Soc. Fr. Mineral. Crystallogr.* **93,** 495 (1970).
3. J. Guillevic, J. Y. Marouille, and D. Grandjean, *Acta Crystallogr. Sect. B* **30,** 111 (1974).
4. R. Chevrel, M. Sergent, J. L. Meury, Dang Tran Quan, and Y. Colin, *J. Solid State Chem.* **10,** 260 (1974).
5. J. P. Troadec, D. Bideau, J. L. Meury, and Dang Tran Quan, *J. Solid State Chem.* **16,** 373 (1976).
6. J. L. Meury, D. Bideau, G. Rosse, J. P. Troadec, and Dang Tran Quan, *Phys. Lett. B* **55,** 375 (1976).
7. H. Wada, M. Onoda, H. Nozaki, and I. Kawada, *J. Less-Common. Met.* **113,** 53 (1985).
8. Y. Ueda, K. Kosuge, M. Urabayashi, A. Hayashi, S. Kachi, and S. Kawano, *J. Solid State Chem.* **56,** 263 (1985).
9. I. Kawada and H. Wada, *Phys. B & C (Amsterdam)* **105,** 223 (1983).
10. H. Nakazawa, K. Tsukimura, H. Hirai, and H. Wada, *Acta Crystallogr. Sect. B* **39,** 532 (1983).
11. T. Sakurai, "Universal Crystallographic Computation Program System (UNICS)," The Crystallographic Society of Japan, 1967.
12. K. Kato, private communication.
13. G. H. Moh, *in* "Topics in Current Chemistry," Vol. 76, p. 108, Springer-Verlag, Berlin, 1978.
14. H. F. Franzen and T. J. Burger, *J. Chem. Phys.* **49,** 2268 (1968).
15. F. Gronvold, H. Haraldsen, B. Pedersen, and T. Tufte, *Rev. Chim. Mineral* **6,** 215 (1969).
16. A. B. De Vries and F. Jellinek, *Rev. Chim. Mineral* **11,** 624 (1974).
17. F. A. Shunk, "Constitution of Binary Alloys," McGraw-Hill, New York, 1969.
18. H. F. Franzen and G. A. Wiegers, *J. Solid State Chem.* **13,** 114 (1975).
19. Y. Oka, K. Kosuge, and S. Kachi, *J. Solid State Chem.* **23,** 11 (1978).
20. I. Kawada, M. Nakano-Onoda, M. Ishii, M. Saeki, and M. Nakahira, *J. Solid State Chem.* **15,** 246 (1975).
21. R. De Jonge, T. J. A. Popma, G. A. Wiegers and F. Jellinek, *J. Solid State Chem.* **2,** 188 (1970).
22. A. B. De Vries and C. Haas, *J. Phys. Chem. Solids* **34,** 651 (1973).
23. P. Poix, *C.R. Acad. Sci. Paris, C* **277,** 1017 (1973).
24. Yu. D. Tretyakov, I. V. Gordeev, and Ya. A. Kesler, *J. Solid State Chem.* **20,** 345 (1977).
25. G. Fatseas, J. L. Meury, and F. Varret, *J. Phys. Chem. Solids* **42,** 239 (1981).